

Preparation and Studying the Optimum Performance for Both CuO and CeO₂ as A Metal Oxide Nanoparticles Catalyst for Synthesis of Glycerol Carbonate from Reaction of Glycerol with Carbon Dioxide Gas

Jassim Mohamed Hamed AL-Kurdhani^{1,3,*}; Huajun Wang^{1,2} and Taha Seham Ismail³

¹ Key Laboratory for Material Chemistry for Energy Conversion and Storage, Ministry of Education, School of Chemistry and Chemical Engineering, Huazhong University of Science and Technology, Wuhan 430074, PR China

² Hubei Key Laboratory of Material Chemistry & Service Failure, Huazhong University of Science and Technology, Wuhan 430074, PR China.

³ Industrial research and development directory - Ministry of sciences and technology, Baghdad - Iraq

* Corresponding author: E-mail: jassim_khay@yahoo.com, Tel.: +86 13164696930.

Abstract:

Two important types of metal oxide nanoparticle catalysts Copper (II) oxide (CuO) and Cerium oxide (CeO₂) are prepared by a suitable method which was traditional precipitation (PT) method at calcination temperature of 400°C for 5h and used for the synthesis of glycerol carbonate GC (C₄H₆O₄) from the direct reaction by the carbonylation of Glycerol GL (C₃H₈O₃) with Carbon Dioxide. The precipitation (PT) was an important route for the preparation of nanoparticles catalyst. The effects of performance of (CuO and CeO₂) nanoparticle catalysts on the conversion of glycerol GL, yield of glycerol carbonate GC, selectivity of glycerol carbonate are researched. XRD, XPS, BET, FT-IR, CO₂-TPD, H₂-TPR are used for the characterization of the prepared catalysts. Comparing the optimal performance between them under reaction conditions were 150 °C, 4MPa (40 bar.), 5h, and both CuO and CeO₂ catalyst amount 37.6 % (based on ratio of glycerol weight) by using 2-pyridinecarbonitrile (C₆H₄N₂) as dehydrating agent and dimethylformamide (DMF), (C₃H₇NO) as solvent. The glycerol conversion (X_{GL}), glycerol carbonate yield (Y_{GC}) and glycerol carbonate selectivity (S_{GC}) over 0.7g CuO are 57.151%, 47.524%, and 83.156%, respectively, and glycerol carbonate yield over 0.7 CeO₂ is 36.2185% or 35.076%, and the yield of GC could reach as high as 78.234% over 1.73g CeO₂, the both catalysts could be easily regenerated by washing with methanol and water after a reaction and then dried at 60 °C overnight after that calcination at 400°C for 5h without loss of activity after five recycling times, In addition to, the (ICP- MS) results confirmed that the leaching of CuO and CeO₂ was below the detection limit.

Keywords: carbonylation of glycerol; glycerol carbonate; CO₂; nanoparticle catalyst; CuO; CeO₂.

1. Introduction

Glycerol carbonate (GC) was a high value-added derivatives but Glycerol (GL) was by-product of biodiesel manufacture, is available in a great quantity, it is predicted that the global production capacity of biodiesel will reach 50 million tons a year in 2020. Because of rapidly increasing production of global biodiesel in a great quantity, it becomes a research and study focus to transform GL to value-added chemicals. One of the derivatives of GL is the glycerol carbonate (GC), GC has a number of science and industrials applications such as a polar high boiling solvent, chemical intermediates, a surfactant component, carrier in batteries, lubricating oils, monomer for polymers and as components for gas separation membranes.[1-5]

GL can be converted to GC by several routes, indirect and direct routes. For the direct route (GL converted to GC by carbonylation with CO₂ by using suitable catalyst), Among this method, the most suitable industrial process for producing GC is the carboxylation of GL with CO₂ due to the non-toxic raw material, mild operation condition, high selectivity of GC and simple purification of GC.[6-8]

The first work attempt was carried out by Vieville et al. [9] using GL and CO₂ gas under supercritical conditions as reactants in the presence of zeolites and basic ion-exchange resins as catalyst, when adding the co-reactant materials such as ethylene carbonate, could GC be formed. Even though the yield of GC could reach 32%, there was no evidence about the direct insertion of CO₂. Also the metal-impregnated zeolite [10] and Tin complexes [11] were reportedly for the carboxylation of glycerol with CO₂, but the conversion of glycerol was not high came to only 2.5% (180 °C, 5 MPa, 6 h) and 5.8% (180 °C, 10 MPa, 3 h), respectively. Thermodynamic calculations showed that the low conversion of GL to GC was because of the number of equilibrium limitations [12], so dehydrate should be used to change the thermodynamic limit. 13X type of zeolite and acetonitrile were employed for this purpose with both Cu/La₂O₃ [13], Bu₂SnO [14] and achieved to a good result. Despite of all these improvements, the conversion of GL is still relatively low and it is a challenge to improve and develop new effective catalytic system.

Currently, the broad and suitable availability of glycerol at low prices, together with the need of new and good economic synthetic routes for chemicals starting from non-petrochemical sources, have created a huge interest in glycerol molecule as a building block, mainly because of the very broad spectrum of its valuable derivatives [7].

To produce GC from GL with dimethyl carbonate (DMC) by transesterification of GL process can be obtained high conversion and high yield by using a suitable catalyst such as alkali metal or carbonate or hydroxide (for example, K_2CO_3 , KOH, NaOH), Ma/Al/Zr mixed oxide, Mg/Al hydrotalcite, calcium diglyceroxide, alkaline earth metal oxide (CaO) and others [7, 15-19].

Nano metal oxide heterogeneous catalysts are a technologically very important as acid-base and unique redox properties such as (La_2O_3 , CeO_2 , NiO, CuO and Co_3O_4 and others).[20]

As the heterogeneous catalysts, Nano metal oxide catalysts performance showed excellent in some catalytic reactions, such as CeO_2 in reduction of carboxylic acid [21], dehydration of alcohols [22] and in alkylation of aromatic compounds [23], Honda et al. 2014 used CeO_2 as the catalyst for the production of various cyclic carbonates from diols and CO_2 with 2-pyridinecarbonitrile as dehydrating agent [24]. Recently, Jiexiong Liu et al. 2016 used CeO_2 as the Nano catalyst for the production GC from GL and CO_2 by carbonylation reaction [25].

Kankanit Phiwdang, et al. 2013 [26], reported that the Catalyst preparation CuO nanostructures catalysts by traditional Precipitation (PT) method using copper chloride ($CuCl_2$) and copper nitrate ($Cu(NO_3)_2 \cdot 3H_2O$). First, each precursor was dissolved in 100 ml deionized water to form 0.1M concentration. NaOH solution (0.1 M) was slowly dropped under vigorous stirring until pH reached to 14. Black precipitates were obtained and repeatedly washed by deionized water and absolute ethanol for several times till pH reached 7. Subsequently, the washed precipitates were dried at 80 °C for 16 h. Finally, the precursors were calcined at (400-500) °C for (4-5) h.

In our present work, we prepared and employed two type of metal oxide nanoparticle (CuO and CeO_2) as the catalyst for the synthesis of GC from GL and CO_2 in the presence of (2-pyridinecarbonitrile) which was used as a dehydration agent to pull water from the middle of the chemical reaction as side product and shift the chemical equilibrium to the GC production side and solvent of CO_2 (Dimethylformamide (DMF)). The important objective of this work was to compare the optimal performance among them (CeO_2 and CuO) as a best of optimal performance, and develop a new effective catalytic system (carbonylation system) to increase the reaction rate and selectivity of the carbonylation of GL. The stability and activity of the suitable catalysts were studied in detail. From our knowledge, this is the first work of the application of (CuO-PT) prepared (Nano particles metal oxide)-based catalyst for using in the GL carbonylation for GC production.

2. Experimental Section.

2.1. Chemicals.

Cerium nitrate hex hydrate $[\text{Ce}(\text{NO}_3)_2 \cdot 6\text{H}_2\text{O}] \geq 90\%$ purity, Copper(II) nitrate trihydrate $[(\text{Cu}(\text{NO}_3)_2 \cdot 3\text{H}_2\text{O})]$ 99% purity, (25 wt.%) ammonia solution (NH_3), Glycerol GL ($\text{C}_3\text{H}_8\text{O}_3$) 99% purity and N,N Dimethylformamide(DMF) ($\text{C}_3\text{H}_7\text{NO}$) 99% purity were bought from Sinopharm Chemical Reagent Co., Ltd., Beijing-China. 2-pyridinecarbonitrate ($\text{C}_6\text{H}_4\text{N}_2$) was purchased from Aladdin Industrial Corporation Co., Shanghai-China. Carbon dioxide (CO_2) 99.9% purity was supplied by Sichuan Tianyi Science & Technology Co., Ltd., Sichuan-China. All these chemicals were used without further purification.

2.2. Catalyst preparation method.

The precipitation (PT) method was a suitable route for the preparation of metal oxide nanoparticles catalysts, the amounts of materials depended on the stoichiometric of materials to prepared the metal oxide nanoparticles catalysts:

Metal oxide nanoparticle catalysts, CuO, and CeO_2 , were prepared by the precipitation (PT) method. CuO is used as the example to introduce the method. 7.55 g of copper nitrate ($\text{Cu}(\text{NO}_3)_2 \cdot 3\text{H}_2\text{O}$) was firstly dissolved in 250 mL of deionized water in a 500mL round bottom 3-neck glass flask (the molar concentration for copper nitrate was 0.125 mol/L), then, the solution was heated to 80 °C by using oil bath and held about 1 h with vigorous stirring. After an appropriate amount of ammonia solution (1.0 mol/L) was added into the mixture, keeping the pH value (10 ± 1), a nanoparticle suspension was formed. The precursor was aged at 60 °C for 1 h, filtered and washed with deionized water for five times, and after that dried at 60°C in vacuum dryer for 2 h, and then grinded to 100 mesh scale, followed by calcination at 400°C for 5 h in air. The obtained product was denoted as CuO-PT-400. Other metal oxide nanoparticle catalysts were also prepared by the same procedure using corresponding salt such as Cerium nitrate hex hydrate $[\text{Ce}(\text{NO}_3)_2 \cdot 6\text{H}_2\text{O}]$ depend on the stoichiometric amount of materials . The samples of metal oxide calcined at 400°C temperatures were named as M_xO_y -PT-400 (400 means the calcination temperature).

2.3. Catalyst characterization

X-ray diffraction (XRD) patterns of the catalysts were measured on a X'Pert PRO using Cu $\text{K}\alpha$ radiation at 30 kV and 15 mA, over a 2θ range of 5-90° with a step size of 0.0167° at a scanning speed of 8min⁻¹.

A Bruker VERTEX 70 FT-IR spectrometer was used to obtain the FT-IR spectra of samples using KBr pellet technique, with 2 cm^{-1} resolution over the wavenumber range $4000\text{-}400\text{ cm}^{-1}$.

The morphology of the particles was observed by use of a scanning electron microscope (SEM, TESCAN VEGA3) with 20.0 kV of an accelerating voltage.

Nitrogen adsorption-desorption isotherms were determined by a volumetric adsorption apparatus (Micrometrics ASAP 2420) at 77K. The surface areas of samples were calculated by using the Brunauer-Emmett-Teller (BET) method. The pore volume was given at $p/p_0 = 0.99$. The pore size distribution was calculated by the Barrett-Joyner-Halenda (BJH) method.

Also, the basicity studies of the prepared catalysts were conducted with temperature-programmed desorption of CO_2 as probe molecule (CO_2 -TPD) using Huasi DAS-7000 apparatus equipped with thermal conductivity detector (TCD). The analysis was performed by heating 100 mg of the catalyst sample under a He flow from room temperature to $800\text{ }^\circ\text{C}$ for 2 h ($10\text{ }^\circ\text{C}/\text{min}$, $50\text{ mL}/\text{min}$). Then, the temperature was decreased to $90\text{ }^\circ\text{C}$, and a flow of pure CO_2 ($50\text{ mL}/\text{min}$) was subsequently introduced into the reactor during 1 h. After the catalyst was swept with (He) for 1 h to remove the physisorbed CO_2 from catalyst surface, the TPD of CO_2 was carried out between $90\text{ }^\circ\text{C}$ and $900\text{ }^\circ\text{C}$ under a He flow ($10\text{ }^\circ\text{C}/\text{min}$, $30\text{ mL}/\text{min}$) and the detection of the desorbed CO_2 was by an on-line gas chromatograph provided with a TCD.

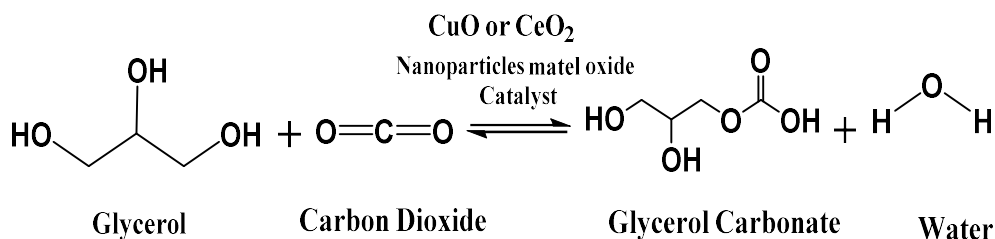
H_2 temperature programmed reduction (H_2 -TPR) measurements were carried out on the CHEMBET 3000 TPR/TPD instrument. Before the reduction, a sample was preheated in a gas ($30\text{ mL}/\text{min}$) at $400\text{ }^\circ\text{C}$ for 30 min to remove surface contaminants. After the sample cooled down to $50\text{ }^\circ\text{C}$, a mixture of 5.01% H_2/Ar was flowing through the reactor and the temperature was increased from $30\text{ }^\circ\text{C}$ to $920\text{ }^\circ\text{C}$. The hydrogen consumption was monitored by a TCD detector.

Inductively coupled plasma mass spectrometry (ICP-MS): Is a type of mass spectrometer capable of detecting minerals and many minerals that are not present at low concentrations such as one part in 10^{15} (part of quadrillion, ppq) on non-overlapping low-contrast isotopes. This is achieved by ionizing the sample using a coupled plasma and then using the mass spectrometer to separate and quantify these ions. For most clinical methods using ICP-MS, there is a relatively simple and rapid preparation process for preparation by acid digestion using $\text{HNO}_3/\text{H}_2\text{O}_2$

mixture to identify metal oxide in sediments using the (ICP-MS) (Varian company production) acid Digestion.

2.4. Reaction procedure.

Glycerol carbonate (GC) was obtained from the carbonylation of glycerol (GL) with CO₂ over nanoparticles catalysts. As shown in scheme 1.



Scheme1. Carboxylation of glycerol with CO₂ over nanoparticles metal oxide catalysts.

The tests of the catalytic activities of the nanoparticles metal oxide catalysts were carried out in a stainless-steel autoclave reactor system with an inner volume of 200ml and it has thermostat with an electric heating jacket, pressure gauge and agitator, the autoclave reactor was one of the most important chemical engineering equipment and its operation is not easy, it requires attention and caution when operating, because it works under conditions of high temperature and high pressure. After ascertaining the validity of the autoclave system (fig.1.), the typical procedure is as follows: 40mmol glycerol (GL), 37mmol% Cat./GL, 16 g of Dimethylformamide (DMF) 6 g of 2-pyridinecarbonitrile, were added into the autoclave together, and then the reactor was sealed, purged with N₂ or CO₂ for 3 times and then pressurized with CO₂ to 4 MPa. Subsequently, the autoclave was heated to the reaction temperature (150 °C) and maintained for certain reaction time (5h) under vigorous stirring. After reaction, the reactor was cooled to room temperature and depressurized, the product mixture was taken out from the autoclave reactor to centrifugal filtration 5000 rpm for 6 min to separation the solid catalyst and liquid products, after that take all liquid product to analyzing.

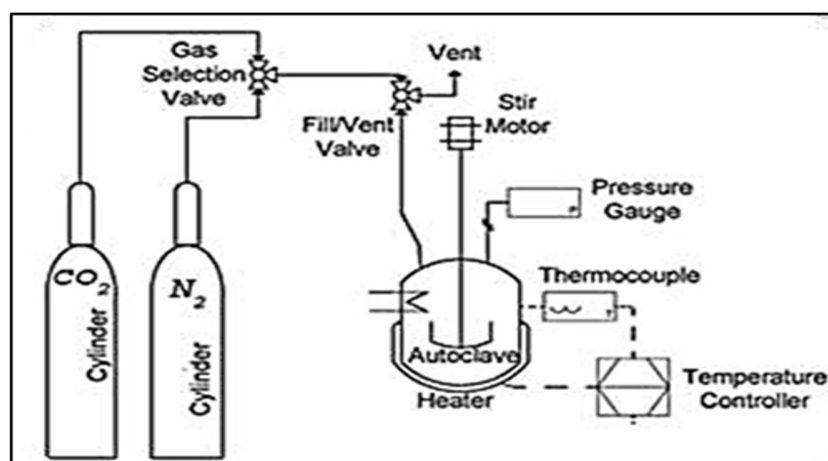


Fig.1. Autoclave reactor system

2.5. Liquid product analysis.

All the components in liquid product were analyzed by the gas chromatograph (Fuli 9790-II) equipped with a flame ionization detector (FID) and a capillary column DM-FFAP (30 m long, 0.25 mm id). The internal standard method was used. Hydrogen (H₂) nitrogen (N₂) (99.999% pure) and air (20.8% O₂, 79.2% N₂), were supplied by (Sichuan Tianyi Science & Technology Co., Ltd., Sichuan, China), air and N₂ were used as the carrier gas with a flow rate of 30 mL/min at 0.4 MPa and H₂ at 0.25MPa. The temperatures of the injector and the detector were 250 C and 270 °C, respectively. The temperature of the column was programmed to have a 2min initial hold at 70 °C, a 15 °C/min ramp from 70 °C to 250 °C and a 15 min hold at 250 °C. A good peak separation was achieved under these conditions for all components. n- Butanol was used as the internal standard to determine Methanol, while tetra ethylene glycol was used as the internal standard to determine GL and GC. Added about 1g methanol to liquid product sample for diluting before injecting into gas chromatograph (Fuli 9790-II), the mass of all sample was (mass of sample + mass of methanol) to determining the mass of GL and GC output with product.

The conversion of GL, X_{GL} , and the yield of GC, Y_{GC} , and selectivity of GC, S_{GC} were calculated according to the following equations:

$$\text{Conversion}(X_{GL}) = \frac{n_{GL.in} - n_{GL.out}}{n_{GL.in}} \times 100 \% \quad (1)$$

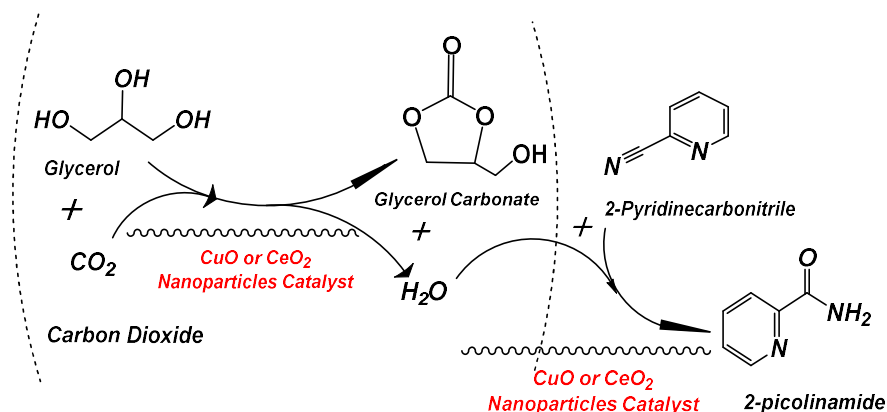
$$\text{yield}(Y_{GC}) = \frac{n_{GC.out}}{n_{GL.in}} \times 100 \% \quad (2)$$

$$\text{Selectivity}(S_{GC}) = \frac{Y_{GC}}{X_{GL}} \times 100 \% \quad (3)$$

Where $n_{GL.in}$ the number of initial moles of GL, $n_{GL.out}$ is the number of moles of GL output (unreacted), $n_{GC.out}$ is the number of moles of GC product.

3. Result and discussion.

The synthesis of GC from GL and CO₂ by carbonylation reaction over metal oxide nanoparticles catalyst in the presence of (2-pyridincarbonitrile), which was used as a dehydration agent to pull water from the middle of the chemical reaction as byproduct to produced 2-picolinamide (C₆H₆N₂O) and shift the chemical equilibrium to the GC production side and solvent of CO₂ Dimethylformamide (DMF). As shown in mechanism of carboxylation reaction in scheme.2. The conditions of reaction were (150 °C temperature, 5h time, and 4MPa initial pressure of CO₂ and 500 rpm of mixing. The Gas chromatography (G.Ch.) analysis of the liquid product mixture out of autoclave reactor is given in Fig.2 it can be found a good peak separation is achieved for all components.



Scheme2. Bath way of carboxylation of glycerol by CO₂ and hydration of 2-cyanopyridine over nanoparticles metal oxide catalysts as the coupling reaction

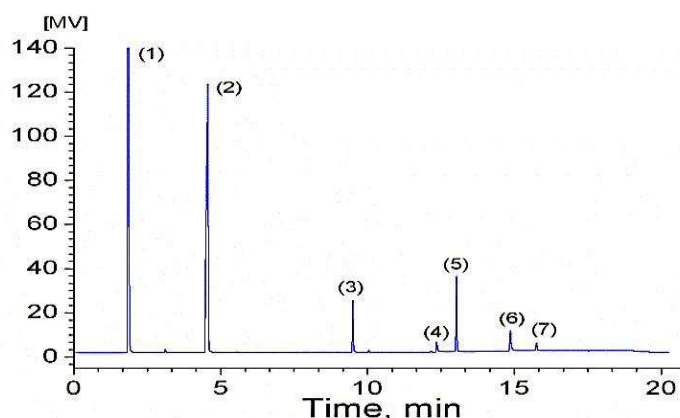


Fig.2 The Gas chromatography analysis peaks of the liquid products mixture ((1) methanol, (2) DMF, (3) 2-pyridincarbonitrile, (4) GL, (5) 2-picolinamide, (6) tetra ethylene glycol, (7) GC.

3.1. Effect of type of nanoparticles metal oxide catalyst.

Two types of metal oxide nanoparticle catalysts (CuO-PT-400) and (CeO₂-PT-400) were used in carbonylation of GL with CO₂ to produce GC and their catalytic performances and presented in table 1. Among two catalysts, the (CuO-PT-400) nanoparticle has the highest catalytic performance; in contrast, CeO₂-PT-400 shows the lowest activity for the reaction of GL with CO₂. Over (CuO-PT-400) catalyst, the GL conversion (X_{GL}), GD yield (Y_{GC}), and GD selectivity (S_{GC}) were determined by equations (1, 2, 3) and we could reach 57.151%, 47.524%, and 83.156%, respectively as shown in table.1. The results mean (CuO-PT-400) nanoparticle is a good catalyst for carbonylation of GL with CO₂.

Table.1

The catalytic performances of the metal oxide nanoparticle catalysts in the carbonylation of GL with CO₂ to produce GC^a.

Cat.	X _{GL} /%	Y _{GC} /%	S _{GC} /%	Ref.
CuO-PT-400	57.151	47.524	83.156	This work
CeO ₂ -PT-400	51.097	36.218	70.88	This work
^b CeO ₂ -PT-400	-	35.076	-	[25]

^a Reaction condition: 40 mmol GL, 0.7g Cat. (Cat/GL=19%), 5 g of 2-pyridinecarbonitrile, 15g DMF, 150 °C, 4 MPa CO₂ and 5h.

^b The results from Y_{GC}/% were calculated as (cat./GL=36.9%), 0.34 g CeO₂ cat., from ref. J. Liu, et al. 2016 [25].

The catalytic performances were presented in Table1. Show conversion of GL., optimal yield of GC and optimal selectivity of GC with (CuO-PT-400) Nano catalyst when compared with (CeO₂-PT-400) and yield of (CeO₂-PT-400), results from Ref. Jiaxiong Liu, al.et [25] ranked as:

$$(\text{CuO-PT-400}) > (\text{CeO}_2\text{-PT-400}) > (\text{CeO}_2\text{-PT-400})_{\text{from J. Liu, al.et [25]}}$$

And the (CuO-PT-400) was more activity than (CeO₂-PT-400) catalysts at 0.7 g catalyst/40 mmol GL.

3.2. Effect of reaction conditions

The effect of reaction conditions over (CuO-PT-400) nanoparticle catalyst as reaction temperatures, CO₂ pressure, time of reaction and amount of catalyst all had investigated in our research and were shown the results in Fig.3 (a-d) and the optimal performances of reaction conditions had shown in Table.2.

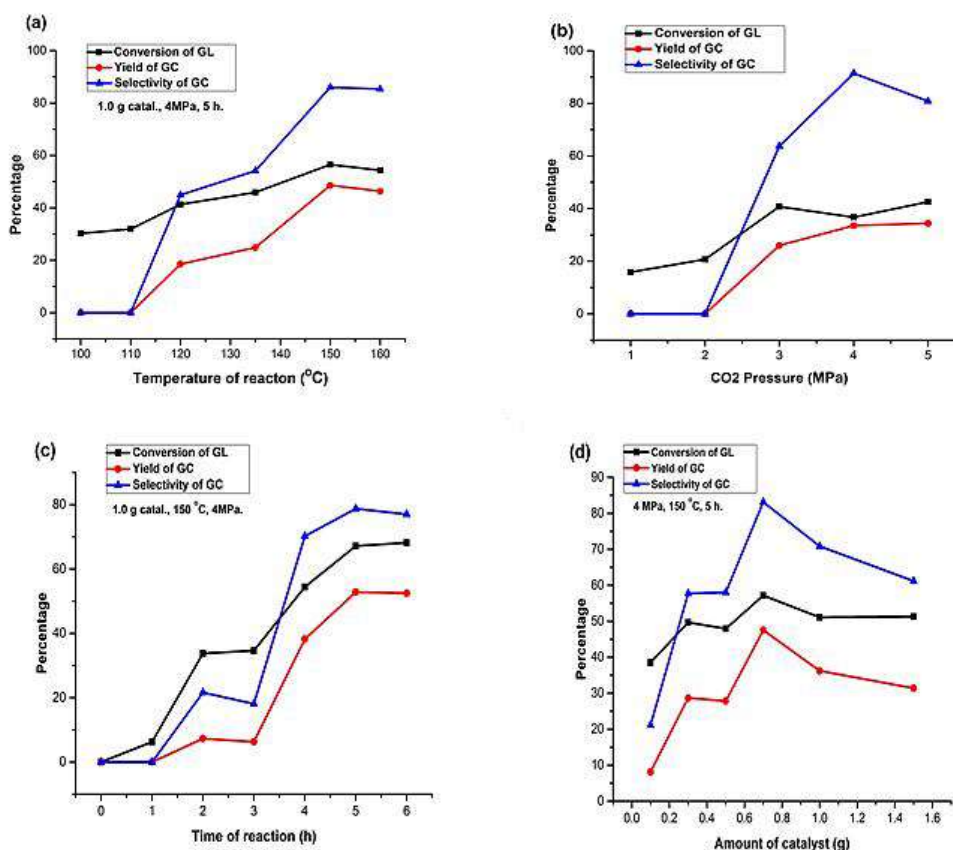


Fig. 3 Effect of (a) reaction temperature, (b) pressure of CO₂, (c) reaction time, and (d) weight of catalyst on carbonylation of GL with CO₂ over CuO-PT-400 catalyst (Reaction condition: 40 mmol GL, 0.7 g Catalyst (Cat/GL=19%), 5 g of 2-cyanopyridine, 15 g of DMF, 150 oC, 4 MPa CO₂ and 5.0 h)

And from article J. Liu, et al. 2016 [25], the effect of reaction conditions over (CeO₂-PT-400) nanoparticle catalyst as reaction temperatures, CO₂ pressure, time of reaction and amount of catalyst had investigated in this research [25] and all the results were shown in Fig.4 (a-d) and the optimal performances of reaction conditions had shown in Table.3.

The above results are found in the Fig.3 (a-d) and Table.2 that perform optimally of (CuO-PT-400) nanoparticle catalysts was T=150 °C, P_{CO₂} = 4 MPa, t_{reaction}= 5h and m_{catal} = 0.7g, the results of conversion of GL (X_{GL}/%), yield of GC (Y_{GC}/%) and selectivity of GC (S_{GC}/%) were 57.1507, 47.5240, and 83.1556 respectively. But the results in the Fig.4 (a-d) and Table.3 (J. Liu, et al. 2016) [25] found perform optimally of (CeO₂-PT-400) nanoparticle catalyst was T=150 °C, P_{CO₂}= 4 MPa, t_{reaction}=5h and m_{Catal.} =0.7g, the results of yield of GC (Y_{GC}/%) is 33.786 and the mass ratio CeO₂ /GL =0.72 and when using 1.73g CeO₂ as the mass ratio CeO₂ /GL =1.9 the results of yield of GC (Y_{GC}/%) is 78.234. But from the economic side when using

0.7g of (CuO-PT-400) the yield of GL $Y_{GC}/\% = 47.5240$ and the mass ratio CuO /GL =0.19, therefore the Optimal performance for (CuO-PT-400) was higher than for (CeO₂-PT-400) in these conditions.

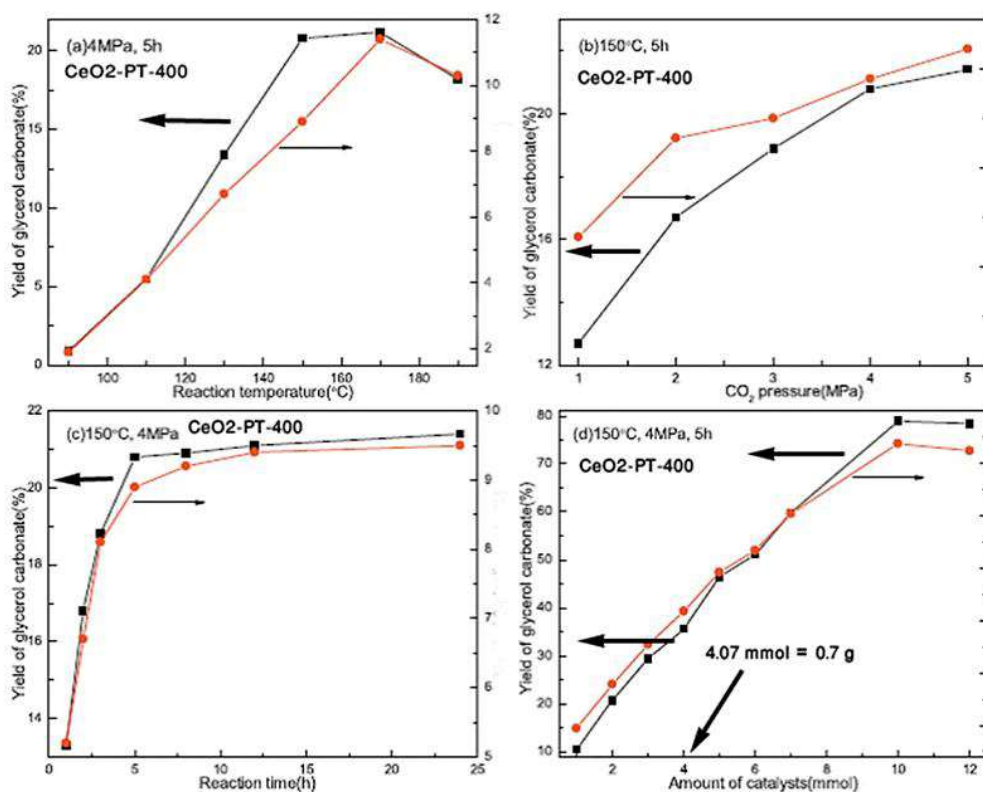


Fig. 4 Effect of (a) reaction temperature, (b) CO₂ pressure, (c) reaction time, (d) amount of catalyst on carbonylation of glycerol with CO₂ over CeO₂-PT-400 (Reaction condition: 10 mmol (0.91g) glycerol, 30 mmol 2-cyanopyridine, 0.34 g CeO₂ for (a), (b) and (c), 10 mL DMF), results from J. Liu, et al. [25]

Table.3 The catalytic performances of the CeO₂-PT-400 nanoparticle catalysts in the carbonylation of GL with CO₂ to produce GC ^a

the optimal performances of reaction conditions	Yield of GC ($Y_{GC}/\%$)
T=170 °C ,Fig.4a	22.354
P _{CO2} =5MPa ,Fig.4b	21.456
Time = 20h ,Fig.4c	35.076
m _{cata.} =1.73g (10)mmol ,Fig.4d	78.234
m _{cata.} =0.7g (4.07mmol) ,Fig.4d	33.786

^a. The results were calculated from J. Liu, et al. 2016 (charts). [25]

Table.4 the amount of CO₂ adsorption and H₂ consumption of CuO-PT-400 nanoparticle catalysts measured respectively by CO₂-TPD and H₂-TPR

Cat.	^a CO ₂ adsorption amount (μmol/g)			Total amount	H ₂ consumption (mmol/g)
	<200 °C	200~380 °C	>380 °C		
CuO-PT-400	13.80(27.3%)	15.00(29.7%)	21.70(43.0%)	50.49	1.66
^b CeO ₂ -PT-400	-	-	-	55.00	^c 0.072

^a. The number in bracket is the percentage of different strength basic sites on total CO₂ desorption amount.

^b. The results of CeO₂-PT-400 were calculated from J. Liu, et al. 2016 [25].

^c. 72 μmol/g from J. Liu, et al. 2016 [25].

3.3 Catalyst characterization.

3.3.1 XRD.

Fig.5, 6 shows the XRD patterns of (CuO, CeO₂ and CeO₂ from work of Ref. [25]) nanoparticles catalysts calcined at temperature (400 °C) for 4h. The samples present a typical band of CuO phase with monoclinic crystal system Ref. Code(00-048-1548) (at 2θ = 32.5, 35.5, 38.8, 46.2, 48.8, 51.4, 53.5, 58.3, 61.5, 66.3, 68.13, 72.5, 75.1, 80.1, 82.5, 83.1, 83.6, and see PDF-2....e2004-163835) also a typical band of CeO₂ phase with monoclinic crystal system Ref. Code(00-044-1159) (at 2θ = 28.55°, 33.077°, 47.490°, 56.328°, 59.096°, 69.407°, 76.736°, 79.079°, 88.451°, 95.432°, and see PDF-2....e2004-163835) In Fig. 5, it is also found the diffraction intensity of crystal face for CuO-PT-400 sample (-110, 002, 111, 200, -112, 020, 202, -113, 022, -311, 113, -220, 311, 004, -222, -204, -313, 222, 400, 402) and the diffraction intensity of crystal face for CuO-PT-400 sample (111, 200, 220, 311, 222, 400, 331, 420, 422) indicating the gradual bulk sintering and growth of crystallite size of CuO-PT-400. All the catalysts show clear and sharp peaks of CuO-PT-400 more than CeO₂-PT-400 and the diffraction intensity of crystal face (111) in CuO-PT-400 and in CeO₂-PT-400 were the greatest among all about (91-100)%. The width of the diffraction lines is produced using the smaller grains. The diffraction peaks of nanoparticles CeO₂-PT-400 were broader, which indicates the presence of small particles in the former catalysts and show the particle size is fine, and all the Cu-based, Ce-based metal oxides nanoparticles obtained by calcination at 400°C for 5h. Exhibit the diffraction peaks of CeO₂ crystals in another article J. Liu, et al. 2016 [25], located at (2θ) around 38.484°, 33.273°, 47.756°, 56.236°, 59.346, 69.254, 69.685, 77.324, and 79.249°, which are attributed to the (111), (200), (220), (311), (222), (400), (331), (420) and (422) reflections, respectively in fig.6. It means that the effectiveness of the CeO₂-PT-400 was a little and less than CuO-PT-400, which is accordant with the order of the catalytic activity for these catalysts (Table 1, except with CuO-PT-400), meaning that the crystal face (111) for CuO-PT-400

nanoparticles catalyst may be have more active site for the carbonylation of GL with CO₂. The predominantly exposed planes were the most stable (111) plane, whereas the CeO₂ and CuO nanoparticles catalyst predominantly exposed the well-defined and less stable (200) and (220) planes. Since the energy required to create oxygen vacancies on the plane has strong relevance with their stabilities, the difference of exposed plane might have affection the catalytic performance of CuO-PT-400 and CeO₂-PT-400 nanoparticles catalyst.

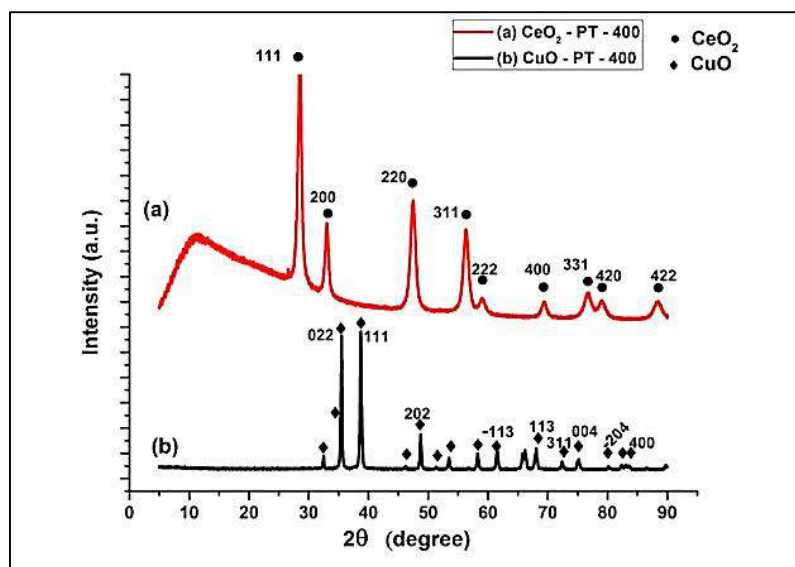


Fig.5 XRD patterns of the nanoparticle catalysts: (a) CeO₂-PT-400, (b) CuO-PT-400.

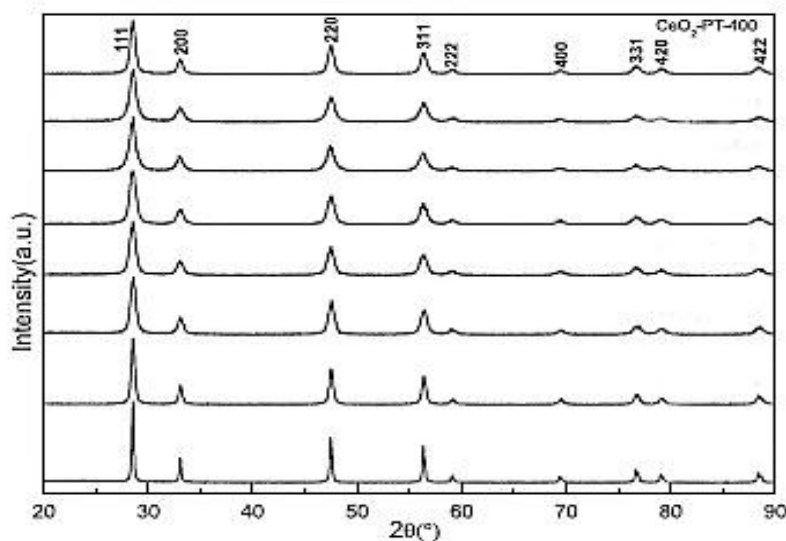


Fig.6 XRD patterns of the nanoparticle catalysts of CeO₂-PT-400 results from J. Liu, et al. 2016 [25]

3.3.2 CO₂-TPD

The basicity of CuO nanoparticle catalysts is characterized by CO₂-TPD and the profiles are shown in Fig. 7. In the TPD profiles of these samples, the peaks at the temperature range of 50~277 °C, 277~490 °C, and > 490 °C are attributed to desorption of CO₂ from weak, medium, and strong basic sites, respectively. By integrating these peak areas shows that except the medium basic sites, the amounts of weak and strong basic sites increase with the increase of calcination temperature and the total amounts of the basic sites as well as. The results mean that the quantitative distribution of different strength basic sites and total amount of desorbed CO₂ are dramatically influenced by the calcination temperature.

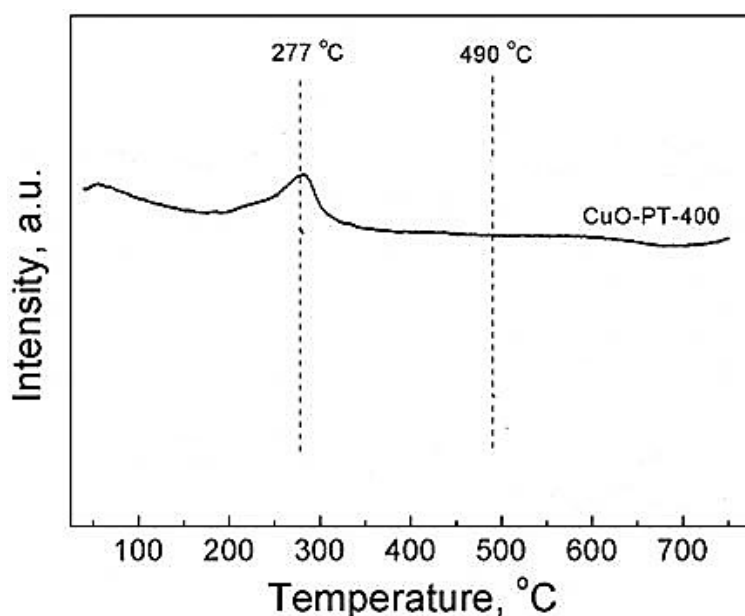


Fig.7. CO₂-TPD profiles of CuO-PT-400 nanoparticles catalyst

From the J. Liu, et al. 2016 results [25] found the basicity of CeO₂ was characterized by CO₂-TPD, and the profiles were shown in Fig. 8. The amount of weak, medium and strong basic sites were estimated from the integrated area under CO₂-TPD profiles in the temperature range of (20–200) °C, (200–450) °C and > 450°C, respectively. It is notice able that the quantitative distribution of different strength basic sites and total amount of desorbed CO₂.

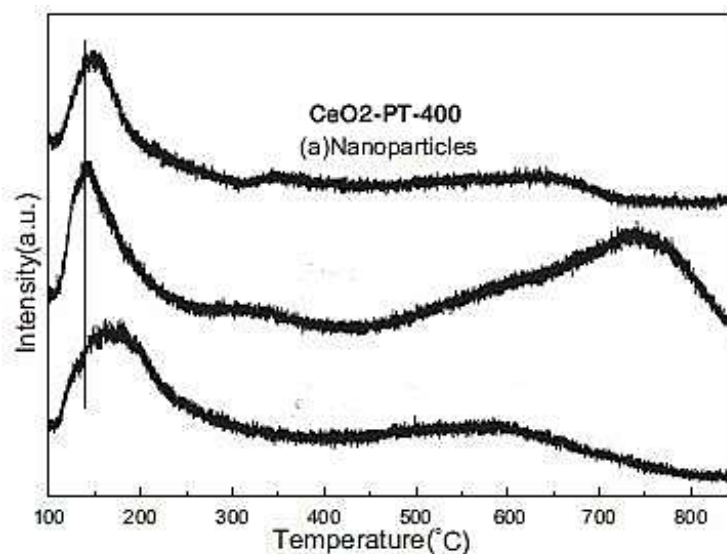


Fig.8. (a) CO₂-TPD profiles of CeO₂-PT-400 nanoparticles catalyst only (a) from J. Liu, et al. 2016 [25]

By integrating these peak areas, the amounts of basic sites can be evaluated and the results are presented in Table 4.

In general, a more basicity is beneficial for the carbonylation of GL with CO₂. Compared with CuO-PT-400 and CeO₂-PT-400 has higher amount of basic sites, so it also has higher GC yield. It is also observed that among these samples, though CeO₂-PT-400 has the highest basicity.

3.3.3 H₂-TPR

The H₂-TPR was used to determine the redox ability and oxygen vacancy density of CuO-PT-400 nanoparticle catalysts in our present work compared with CeO₂-PT-400 nanoparticle catalysts in the J. Liu, et al. 2016 [25]. The H₂-TPR profiles of CuO and CeO₂ are shown in Fig. 8 and Fig. 9; the data of H₂ consumption at 400 °C are listed in the sixth column in Table 3. It is found that all of the samples have only one strong and sharp reduction peak, indicating that there may be a type of CuO and CeO₂ species in these samples. Meanwhile, in these H₂-TPR profiles, the temperature of H₂ consumption maximum is different and it was 277 °C for CuO-PT-400. In these samples, CuO-PT-400 has the lowest reduction temperature, meaning this sample can be easily reduced.

The H₂-TPR characterization can be engaged to determine the redox ability and oxygen vacancy density of CeO₂. The H₂-TPR profiles of CeO₂ are depicted in Fig. 9 and the data of H₂ consumption below 600°C is listed in Table 3. Two obvious peaks could be observed from the

reduction profiles: the low-temperature peak at about 540°C and the high-temperature peak at about 890°C. The peak below 600°C is generally interpreted as the surface shell reduction, including the reduction of the surface Ce from Ce⁴⁺ to Ce³⁺ and the formation of bridging OH¹⁻ groups, and the peak above 600°C is corresponding to the bulk reduction [25].

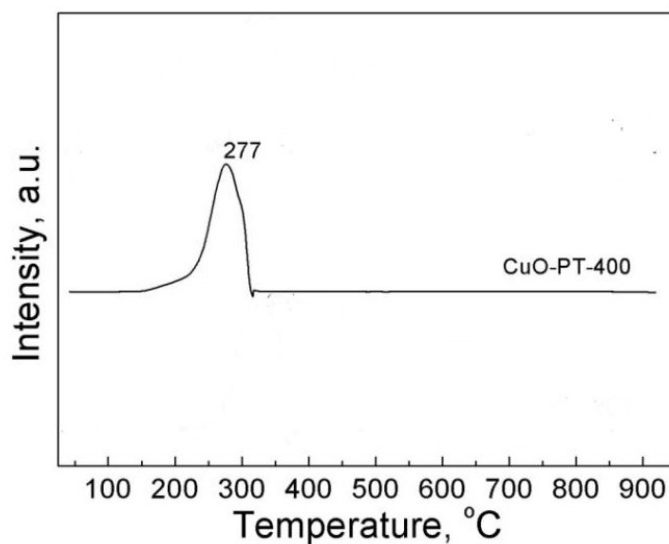


Fig.9 H₂-TPR profiles of the CuO-PT-400 nanoparticle catalysts calcined at temperature 400 °C, in our work.

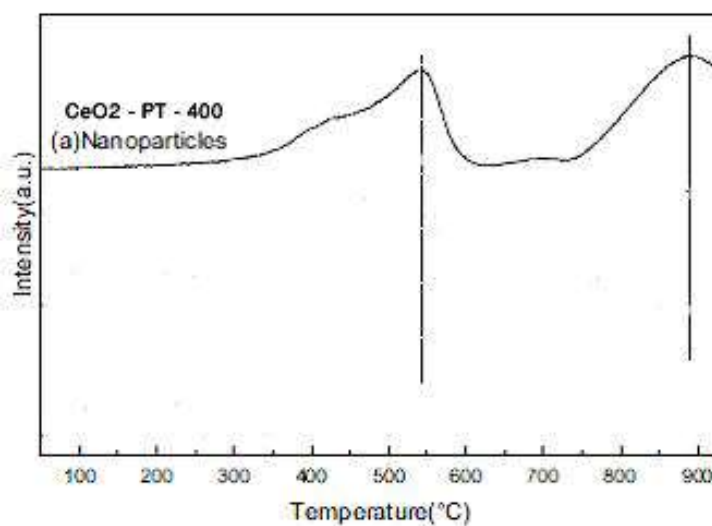


Fig.10 H₂-TPR profiles of the CeO₂-PT-400 nanoparticle catalysts only (a) calcined at temperature 400 °C, from the J. Liu, et al. 2016 results [25]

These differences may be due to the difference of the particle size, surface area and morphology with various exposed crystal planes. The H₂ consumption can be a glancing

representative of oxygen vacancy density and decreases with the increase of the calcination temperature (see the sixth column in Table 3), suggesting that CuO-PT-400 may have the highest oxygen storage/release capacity and CeO₂-PT-400 has the lowest. In the present work, we have found that the catalytic activity of CuO nanoparticle catalyst is connected to not only its amount of basic sites and surface area, but also the redox ability and oxygen vacancy density. CuO-PT-400 with the best redox ability and a higher oxygen vacancy gives the highest yield of GC. In contrast, CeO₂-PT-400 produces the lowest GC yield by using the same amount of catalyst (0.7g) because of the least oxygen vacancy and the weakest redox ability. On the basis of these understanding, it is not unreasonable to predict that the best catalyst for the synthesis of GC from carbonylation of GL with CO₂ should have not only high amount of basic sites and surface area, but also high redox ability and oxygen vacancy.

3.3.4 XPS

Fig.11. Presents the X-ray photoelectron spectroscopy (XPS) of (CuO-PT-400) nanoparticles catalyst Survey scan. All the indexed peaks are corresponding to Cu, O and C, as shown in the survey spectrum, the spectrum shows Cu photoelectron peaks (Cu 2p), O peaks (O 1s) and C peaks (C 1s). The high resolution XPS spectra of the (Cu 2p), (O 1s) and (C 1s) are shown in Figure.11. The fitting peaks were strong at about (634.002, 529.852 and 285.002) eV for (Cu 2p, O 1s and C 1s) respectively. Also the high resolution XPS spectra of the Cu 2p were higher one peaks lie at 933.31 eV. And the O1s was core-level. The spectrum is broad and consists of two levels of peaks, at the lower level binding energy of 528.65 eV which is in agreement with O⁻² in copper oxide while the other level peak at a higher energy of 529.85 eV accredited to adsorbed oxygen on the surface of nanoparticles. The results are in agreement with the literature [27]. The atomic ratio of Cu:O calculated on the basis of Cu 2p and O 1s spectra is approximately equal to 3:4, which shows that the surface of the product is rich in O, but the C 1s with higher one peaks lie at 285.002 eV and very little at (CuO-PT- 400) nanoparticles catalyst. No peaks of other elements except C, Cu and O were observed in the picture, indicating the high purity of the product.

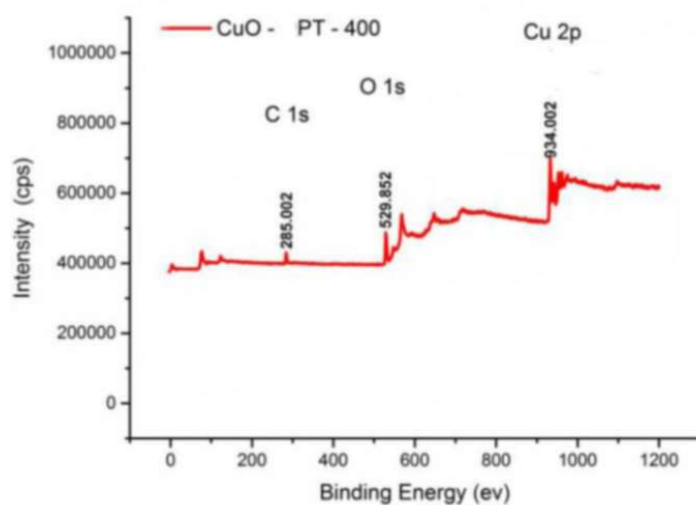


Fig.11. X-ray photoelectron spectroscopy (XPS) of (CuO –PT–400) nanoparticles catalyst Survey scan in the our work

In order to reveal the chemical state of cerium on the catalyst surface, the three as-prepared CeO₂ samples were investigated by XPS. The XPS patterns of Ce (3d) and O (1s) region are illustrated in Fig. 12. From the J. Liu, et al. 2016 results [25]. The O (1s) spectra was composed of two overlapping peaks. The main peak with lower binding energy of 529.1eV roots in the lattice oxygen with Ce⁴⁺ ions [28]. The lower intense peak at 531.2 eV was assigned to different attributions: CO₃²⁻ contamination [29], hydroxyl contamination [30], highly polarized oxygen around the defect site [31] and oxygen vacancies in metal oxides [28].

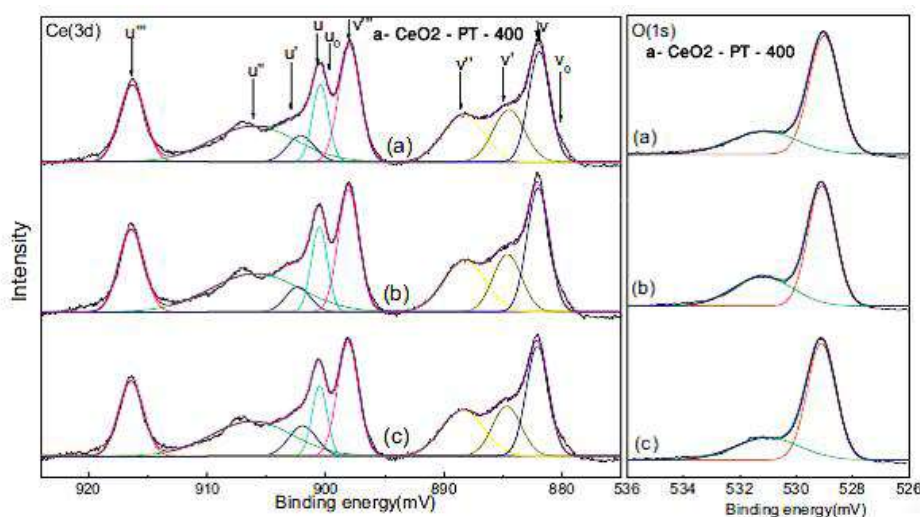


Fig.12. X-ray photoelectron spectroscopies (XPS) of (CuO –PT–400) nanoparticles catalyst only (a) Survey scan from the J. Liu, et al. 2016 results [25]

3.3.5 Nitrogen adsorption–desorption isotherms analysis (BET)

The catalysts showed large BET surface areas: 58.54 m²/g and 59.40 m²/g for nanoparticles catalyst, (CuO-PT-400) and (CeO₂-PT-400), respectively, as listed in Table 5. Compared with the other two type of nanoparticles catalyst, (CuO-PT-400) and (CeO₂-PT-400) and in the Jiaxiong Liu, et al. 2016 results [25] showed larger surface area and average pore diameter, which was in favor of the activation and diffusion of the reactants. Typically, metal oxide grains grew into nanoparticles catalyst, the dissolution and recrystallization at the crystal-solution interface under hydrothermal condition, which was beneficial of the homogenous morphology and crystallite size.

Table.5:

The BET surface area and pore diameter for the (CuO-PT-400) and ^a(CeO₂-PT-400) nanoparticles catalysts.

Cat.	BET Surface Area (m ² /g)	Average pore diameter (nm)
CuO-PT-400	58.54	7.75
^a CeO ₂ -PT-400	59.40	9.94

^a. From the J. Liu, et al. 2016 results [25].

3.4 Stability of the CuO-PT-400 and CeO₂-PT-400 nanoparticle catalyst.

Stability of CuO-PT-400 nanoparticles catalyst is very important to complete all the functions of using the catalyst and one of these functions is recyclability of catalyst several times at least five times, the used catalysts were recovered. The stability of CuO-PT-400 was also researched and the result is shown in Fig. 13. It is found that at the fourth recycling, the activity of CuO-PT-400 hardly decreases and the GL conversion and GC yield can also reach 46.09% and 37.71%, respectively. At the fifth recycling, the GL conversion and GC yield reach 46.10% and 35.86%, respectively, indicating that the activity of CuO-PT-400 slightly decreases. In order to ascertain the reason of the decrease of the catalytic activity for the CuO-PT-400 catalyst, the recovered CuO-PT-400 in the fifth recycling was also characterized by XRD and FT-IR. Fig.14 (a) shows that the crystalline structure of recovered CuO-PT-400 is changed, and it has a strong cubic Cu phase ($2\theta = 43.5^\circ, 50.65^\circ$, see PDF 00-001-1242). Fig.15 (a) shows that in the FT-IR spectra of recovered CuO-PT-400, the characteristic peaks attributed to Cu-O stretching mode (at 517 and 598 cm⁻¹) are vanished. These results imply that generation of Cu phase is responsible for the deactivation of the CuO-PT-400 catalyst. Interestingly, when the recovered CuO-PT-400 is calcined at 400 °C, its main phase can be converted back into the monoclinic CuO again (Fig. 14 (b), Fig. 15 (b)).

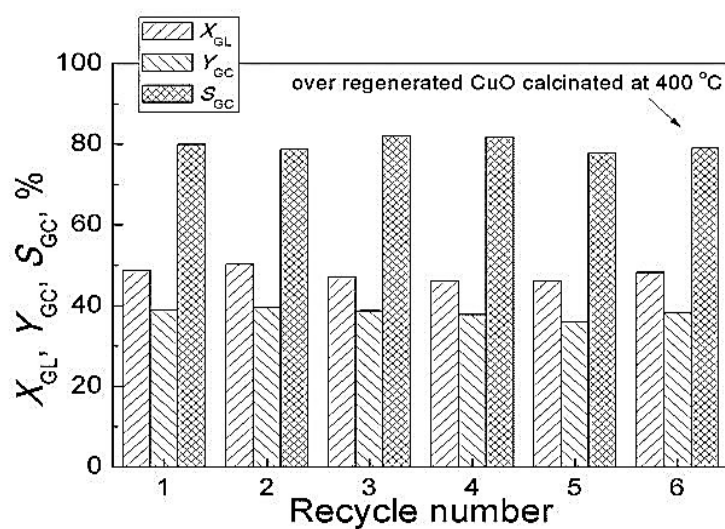


Fig.13. The stability of CuO-PT-400 nanoparticle catalyst on the reaction of GL with CO₂ (Reaction condition: 40 mmol GL, 37.7mmol % Cat./GL, 5 g of 2-pyridinecarbonitrate, 15g DMF, 150 °C, 4 MPa CO₂, 5 h).

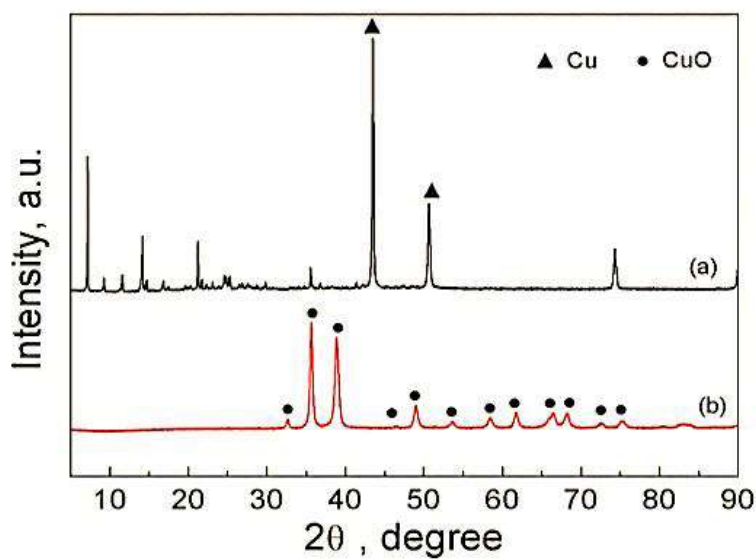


Fig.14. XRD patterns of the CuO nanoparticle catalysts: (a) the recovered CuO-PT-400 catalyst after the fifth recycling; (b) the recovered CuO-PT-400 catalyst regeneration by again calcination at 400 °C.

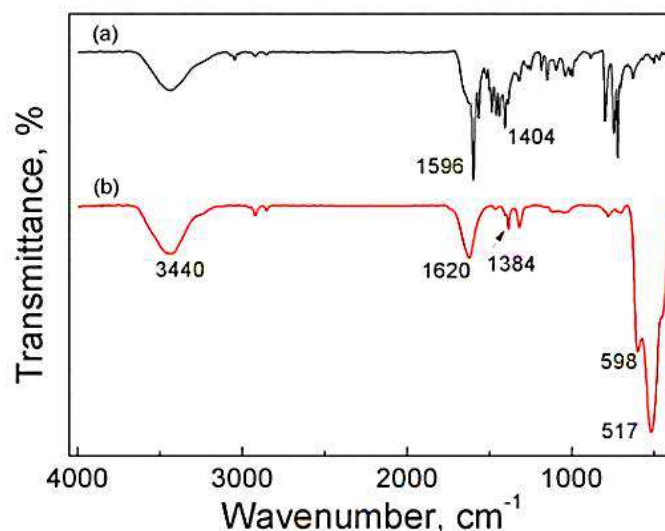


Fig.15. FT-IR spectra of CuO nanoparticles catalysts: (a) the recovered CuO-PT-400 catalyst after the fifth recycling; (b) the recovered CuO-PT-400 catalyst regeneration by again calcination at 400 °C.

Meanwhile, the regenerated catalyst CuO-PT-400 was used to the reaction of GL and CO₂ and also can produce GL conversion of 48.25% and GC yield of 38.10% (Fig. 13). It indicates that the recovered catalyst CuO-PT-400 can be easily regenerated by calcining at 400 °C after washing in methanol three times. Furthermore, the Cu concentration in the reaction mixture in the first run was also measured by inductively coupled plasma-mass spectrometry (ICP-MS) and the result only 45.12 µg/L, indicating that the leaching of CuO almost can be neglected.

In addition; the used CeO₂-PT-400 catalysts in the J. Liu, et al. 2016 results [25], were recovered, washed with ethanol or methanol and dried at 60 °C for 24 h, but they showed great loss of activity (yield of glycerol carbonate was 4.1% for the used CeO₂-PT-400, only 1/4 of the fresh catalyst.). Thus a deactivation of CeO₂ occurred in the CeO₂/2-cyanopyridine/DMF system. One possible reason might be that the produced amide, such as benzamide, was adsorbed on the CeO₂ surface and poisoned the active sites of CeO₂. In order to further investigate the used catalysts, XRD and FT-IR characterizations were conducted. XRD profiles were unchanged for the catalysts before and after the reaction with 2-cyanopyridine as dehydrating agent, suggesting that the nanostructure of CeO₂ was stable under the reaction conditions. The IR spectra of the used catalysts showed no obvious sign of adsorption of amides with respect to that of the fresh one, but the peak of hydroxyl became noticeably larger.

For the recycle use of CeO_2 , the regeneration of spent catalysts was performed by calcination at 400°C for 5 h. The recyclability of CeO_2 nanoparticles was verified as shown in Fig.16. The yield of glycerol carbonate and 2-picolinamide over regenerated CeO_2 stayed practically the same as that of the fresh one even after recirculation for five times[25]. ICP results confirmed that the leaching of CeO_2 was below the detection limit, indicating that the microstructure of the catalyst was stable and the active sites were easily regenerated by a simple calcination procedure [25].

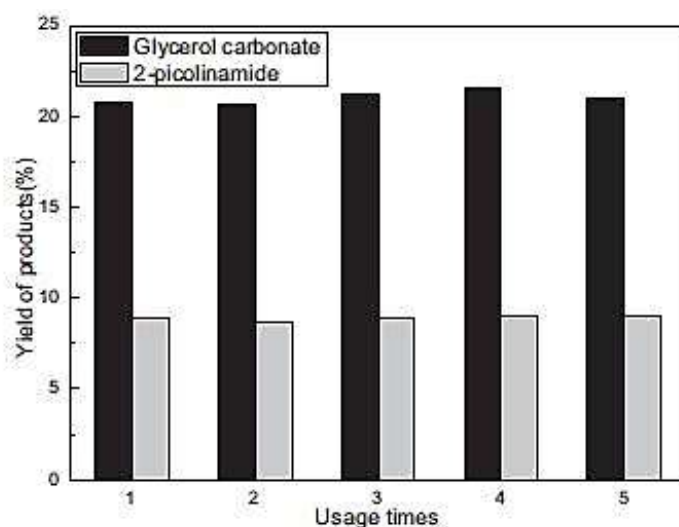


Fig.16 Recyclability of CeO_2 -PT-400 (Reaction condition: 10 mmol glycerol, 30 mmol 2-cyanopyridine, 0.34 g CeO_2 , 10 mL DMF, 150°C , 4 MPa CO_2 , 5 h). From the J. Liu, et al. 2016 results [25]

3.5. Comparison the Optimal performance for both CuO and CeO_2

Comparison the Optimal performance for both CuO-PT-400 and CeO_2 -PT-400 as a metal oxide nanoparticles Catalyst in the carbonylation the Glycerol with Carbon Dioxide to produce Glycerol carbonate by The results of this work which are listed in the (table.6,7) and found at the best reaction conditions (40 mmol GL, 0.7 g Catalyst as the mass ratio $\text{CuO}/\text{GL}=0.19$, 5 g of 2-cyanopyridine, 15 g of DMF, 150°C , 4MPa CO_2 and 5.0 h) the Optimal performance for CuO-PT-400 in conversion of GL, $X_{\text{GL}}/\%$, yield of GC, $Y_{\text{GC}}/\%$ and selectivity of GC, $S_{\text{GC}}/\%$ were 57.1507, 47.5240 and 83.1556 respectively. And in comparison with the results of the (J. Liu, et al. 2016 results) [25] for CeO_2 -PT-400 at the same reaction conditions, found the yield of GC, $Y_{\text{GC}}/\%$ was 33.786, but when using very high amount of CeO_2 1.73g to GL as the mass ratio $\text{CeO}_2/\text{GL}=1.9$ the yield of GC, $Y_{\text{GC}}/\%$ was 78.234 that means the Optimal performance for CuO-PT-400 more than the Optimal performance for CeO_2 -PT-400 under the same reaction conditions.

Comparison the Catalyst characterizations as shown in table.5, it is very clear that the XRD and CO₂-TPD Catalyst characterizations for both CuO-PT-400 and CeO₂-PT-400 were most stable 111 face, high basic sites respectively, but the Catalyst characterizations H₂-TPR and XPS for CuO-PT-400 were (high redox ability and high O₂ vacancy) and (high polarized O₂ with impurity C) respectively, and for CeO₂-PT-400 were (low redox ability and low O₂ vacancy) and (high polarized O₂) respectively, also the BET Surface area (m²/g) for CuO-PT-400 was 58.54 m²/g, and for CeO₂-PT-400 was 59.40 m²/g. Moreover the recyclability for CuO-PT-400 and CeO₂-PT-400 were five times.

Through the above mentioned and according to our knowledge, the optimal performance of CuO-PT-400 and CeO₂-PT-400 are both high and higher than metal oxide nanoparticles Catalyst else in the carbonylation the Glycerol with Carbon Dioxide to produce Glycerol carbonate, but when comparing the overall optimum performance of both CuO-PT-400 and CeO₂-PT-400 (Table.6,7) were very close and when looking closely, the optimal performance of CuO-PT-400 is somewhat better than CeO₂-PT-400 because the catalyst/GL was very suitable less than 20% but over CeO₂-PT-400 good yield of GC with high amount of catalyst/GL was more than 188%.

Table.6

Comparison the Optimal performance for both CuO and CeO₂ as a metal oxide nanoparticles Catalyst in the carbonylation the Glycerol with Carbon Dioxide to produce Glycerol carbonate ^a.

The optimal performances properties	CuO-PT-400 (this work)	CeO ₂ -PT-400 (this work)	^b CeO ₂ -PT-400 (ref.[25])
X _{GL} /%	57.1507	57.1507	-
Y _{GC} /%	47.5240	47.5240	33.786, (78.234) ^c
S _{GC} /%	83.1556	83.1556	-
XRD	Most stable 111	Most stable 111	Most stable 111
CO ₂ -TPD	High basic sites	High basic sites	High basic sites
H ₂ -TPR	High redox ability and O ₂ vacancy	High redox ability and O ₂ vacancy	low redox ability and O ₂ vacancy
XPS	High polarized O ₂	High polarized O ₂	High polarized O ₂ with impurity C
BET	58. 54 m ² /g	58. 54 m ² /g	59. 40 m ² /g
Recyclability	5 times	5 times	5 times

^a Reaction condition: 40 mmol GL, 0.7 g Catalyst (cat/GL=19%), 5 g of 2-cyanopyridine, 15 g of DMF, 150 °C, 4MPa CO₂ and 5.0 h.

^b from the J. Liu, et al. 2016 article results [25].

^c Over 1.73 g Catalyst (CeO₂) and 0.921g GL (cat/GL=188%).

Table.7

Comparison the Optimal performance of mass for both CuO and CeO₂ as a metal oxide nanoparticles Catalyst in the carbonylation the Glycerol with Carbon Dioxide to produce Glycerol carbonate ^a

The Mass of Catalyst (g)	Y _{GC} /% over (CuO-PT-400) (this work)	Y _{GC} /% over (CeO ₂ -PT-400) (this work)	Y _{GC} /% over (CeO ₂ -PT-400) ^b . (ref.[25] work)
0.5	27.8	14.0	28.0
0.7	47.5(cat/GL=19%)	36.0(cat/GL=19%)	35.0(cat/GL=76%)
1.0	36.5	-	48.0
1.73	33.0(cat/GL=46.96%)	-	78.0 (cat/GL=188%)

^a Reaction condition: 40 mmol GL (3.684g GL.), 5 g of 2-cyanopyridine, 15 g of DMF, 150 °C, 4MPa CO₂ and 5.0h.

^b from the J. Liu, et al. 2016 article results for 0.921g GL [25].

4. Conclusion.

CuO and CeO₂ nanoparticle were synthesized by precipitation method (PT). It showed the best two and excellent catalytic optimal performance among nanoparticles metal oxide catalyst in the carbonylation of glycerol and CO₂ with 2-cyanopyridine as a dehydrating agent. The active site of CuO-PT-400 and CeO₂-PT-400 catalysts may be crystal face (111). The incredibly yield of glycerol carbonate GC (can reach about 33-47%) had strong relevance with the efficient hydration of 2-pyridinecarbonitrile (2-cyanopyridine) and solvent effect of DMF and (400) °C was a good calcination temperature for 5h. The proper reaction conditions were (5.0-7.0) g 2-pyridinecarbonitrile (about 3 times of stoichiometric value), 150 °C, 4 MPa and 5 h. The active site of the CuO catalyst is all CuO surface also the CeO₂ catalyst is all CeO₂ surface. The catalyst not only has higher surface area, but also higher mechanical strength, and is suitable for the industrial reactor. The stability research for CuO and CeO₂ nanoparticle shows that the catalyst can be reused five times with little loss of activity and can be easily regenerated by calcination at 400 °C after washing in methanol or ethanol three times. In our future work, the suitable support for this catalyst and mixed this catalyst with another suitable nanoparticles metal oxide catalyst will be investigated and reported in due course and when Comparison the Optimal performance for CuO, CeO₂ in this our work and CeO₂ from J. Liu, et al. 2016 [25] article work found the Optimal performance were very close in low mass of catalyst less than 1g and the Optimal performance of CuO-PT-400 more than CeO₂-PT-400 but at high mass of catalyst more than 1g the Optimal performance of CeO₂-PT-400 more than CuO-PT-400. On the other hand, in chemical engineering and chemical industries, the amount of catalyst must be less than the reactants as the mass ratio catalyst/GL = 0.1 – 0.3, but in J. Liu, et al. 2016 [25] article the

amount of catalyst as the mass ratio $\text{CeO}_2/\text{GL} = 1.88$ (cat./GL=188%) this very high, in our work the amount of catalyst as the mass ratio $\text{CuO}/\text{GL} = 0.19$ (cat./GL=19%) (Table 6, 7).

Economically and industrially: in our work and comparison with results of ref. [25], the optimal performance of CuO-PT-400 more than CeO_2 -PT-400 because the CuO-PT-400 was an economic, efficient and new catalyst for synthesis of glycerol carbonate from glycerol and Carbon Dioxide.

Author Contributions: Formal analysis, Jassim Mohamed Hamed AL-Kurdhani; Funding acquisition, Jassim Mohamed Hamed AL-Kurdhani; Investigation, Jassim Mohamed Hamed AL-Kurdhani; Project administration, Huajun Wang; Resources, Taha Seham Ismail; Software, Jassim Mohamed Hamed AL-Kurdhani; Supervision, Huajun Wang; Writing – original draft, Taha Seham Ismail; Writing – review & editing, Jassim Mohamed Hamed AL-Kurdhani.

Acknowledgements

We acknowledge the financial support by the National Natural Science Foundation of China (21106050), the Specialized Research Foundation for the Doctoral Program of Ministry of Education of China (20100142120066), and the Fundamental Research Funds for the Central Universities of China (2011QN117) for laboratory work at the School of Chemistry and Chemical Engineering and for testing and analysis of materials. XRD and SEM analysis was performed in the Analytical and Testing Center, and FT-IR analysis was performed in the Experimental Teaching Center of chemistry and Chemical Engineering, School of Chemistry and Chemical Engineering, Huazhong University of Science and Technology. Also we acknowledge the financial support by Industrial research and development directory - Ministry of sciences and technology, Baghdad - Iraq. The content is solely the responsibility of the authors and does not necessarily represent the official views of these official institutions

Conflicts of Interest: The authors declare no conflicts of interest.

References

- [1] P. Okoye, B. Hameed, [Review on recent progress in catalytic carboxylation and acetylation of glycerol as a byproduct of biodiesel production](#), Renewable and Sustainable Energy Reviews, 53 (2016) 558-574.
- [2] J.P. da Costa Evangelista, A.D. Gondim, L. Di Souza, A.S. Araujo, [Alumina-supported potassium compounds as heterogeneous catalysts for biodiesel production](#): a review, Renewable and Sustainable Energy Reviews, 59 (2016) 887-894.

- [3] A.P. Vyas, N. Subrahmanyam, P.A. Patel, [Production of biodiesel through transesterification of Jatropha oil using \$KNO_3/Al_2O_3\$ solid catalyst](#), 88 (2009) 625-628.
- [4] G. Baskar, I.A.E. Selvakumari, R. Aiswarya, [Biodiesel production from castor oil using heterogeneous Ni doped ZnO nanocatalyst](#), Bioresource technology, 250 (2018) 793-798.
- [5] F. Moghzi, J. Soleimannejad, [Sonochemical synthesis of a new nano-sized barium coordination polymer and its application as a heterogeneous catalyst towards sono-synthesis of biodiesel](#), Ultrasonics sonochemistry, 42 (2018) 193-200.
- [6] J.R. Ochoa-Gómez, O. Gómez-Jiménez-Aberasturi, B. Maestro-Madurga, A. Pesquera-Rodríguez, C. Ramírez-López, L. Lorenzo-Ibarreta, J. Torrecilla-Soria, M.C. Villarán-Velasco, [Synthesis of glycerol carbonate from glycerol and dimethyl carbonate by transesterification: Catalyst screening and reaction optimization](#), Applied Catalysis A: General, 366 (2009) 315-324.
- [7] P. Lu, H. Wang, K. Hu, [Synthesis of glycerol carbonate from glycerol and dimethyl carbonate over the extruded CaO-based catalyst](#), Chemical engineering journal, 228 (2013) 147-154.
- [8] K. Hu, H. Wang, Y. Liu, C. Yang, [\$KNO_3/CaO\$ as cost-effective heterogeneous catalyst for the synthesis of glycerol carbonate from glycerol and dimethyl carbonate](#), Journal of Industrial and Engineering Chemistry, 28 (2015) 334-343.
- [9] C. Vieville, J. Yoo, S. Pelet, Z. Mouloungui, [Synthesis of glycerol carbonate by direct carbonation of glycerol in supercritical \$CO_2\$ in the presence of zeolites and ion exchange resins](#), Catalysis Letters, 56 (1998) 245-247.
- [10] M. Aresta, A. Dibenedetto, F. Nocito, C. Pastore, [A study on the carboxylation of glycerol to glycerol carbonate with carbon dioxide: the role of the catalyst, solvent and reaction conditions](#), Journal of Molecular Catalysis A: Chemical, 257 (2006) 149-153.
- [11] R.P. Leonardo P. Ozorioa, Luciana da Cruz Machadaa, Jussara L. Mirandab, Cássia C. Turcib, Antônio C.O. Guerrab, E. Falabella Souza-Aguiara, c, Claudio J.A. Mota, , [Metal-impregnated zeolite Y as efficient catalyst for the direct carbonation of glycerol with \$CO_2\$](#) ", Appl. Catalyst., A-Gen. , Volume 504 (5 September 2015) Pages 187–191. Pages 187-191.
- [12] J. Li, T. Wang, [Chemical equilibrium of glycerol carbonate synthesis from glycerol](#), The Journal of Chemical Thermodynamics, 43 (2011) 731-736.
- [13] S. Paulose, R. Raghavan, B.K. George, [Copper oxide alumina composite via template assisted sol-gel method for ammonium perchlorate decomposition](#), Journal of industrial and engineering chemistry, 53 (2017) 155-163.
- [14] J. George, Y. Patel, S.M. Pillai, P. Munshi, [Methanol assisted selective formation of 1, 2-glycerol carbonate from glycerol and carbon dioxide using \$nBu_2SnO\$ as a catalyst](#), Journal of Molecular Catalysis A: Chemical, 304 (2009) 1-7.
- [15] S.C. Kim, Y.H. Kim, H. Lee, B.K. Song, [Lipase-catalyzed synthesis of glycerol carbonate from renewable glycerol and dimethyl carbonate through transesterification](#), Journal of Molecular Catalysis B: Enzymatic, 49 (2007) 75-78.
- [16] J.R. Ochoa-Gómez, O. Gómez-Jiménez-Aberasturi, C. Ramírez-López, M. Belsué, [A brief review on industrial alternatives for the manufacturing of glycerol carbonate](#), a green chemical, Organic Process Research & Development, 16 (2012) 389-399.
- [17] Q.X.L. M.M. Du, W.T. Dong, T. Geng, Y.J. Jiang, , [Synthesis of glycerol carbonate from glycerol and dimethyl carbonate catalyzed by \$K_2CO_3/MgO\$](#) , Res. Chem. In termed, 38 (2012) 1069–1077.
- [18] F.S.H. Simanjuntak, T.K. Kim, S.D. Lee, B.S. Ahn, H.S. Kim, H. Lee, [CaO-catalyzed synthesis of glycerol carbonate from glycerol and dimethyl carbonate: Isolation and characterization of an active Ca species](#), Applied Catalysis A: General, 401 (2011) 220-225.
- [19] M.G. Alvarez, A.M. Segarra, S. Contreras, J.E. Sueiras, F. Medina, F. Figueras, [Enhanced use of renewable resources: transesterification of glycerol catalyzed by hydrotalcite-like compounds](#), Chemical Engineering Journal, 161 (2010) 340-345.

- [20] S. Sato, F. Sato, H. Gotoh, Y. Yamada, [Selective dehydration of alkanediols into unsaturated alcohols over rare earth oxide catalysts](#), ACS Catalysis, 3 (2013) 721-734.
- [21] Y. Sakata, V. Ponec, [Reduction of benzoic acid on CeO₂ and, the effect of additives](#), Applied Catalysis A: General, 166 (1998) 173-184.
- [22] H. Gotoh, Y. Yamada, S. Sato, [Dehydration of 1, 3-butanediol over rare earth oxides](#), Applied Catalysis A: General, 377 (2010) 92-98.
- [23] M. Kobune, S. Sato, R. Takahashi, [Surface-structure sensitivity of CeO₂ for several catalytic reactions](#), Journal of Molecular Catalysis A: Chemical, 279 (2008) 10-19.
- [24] M. Honda, M. Tamura, K. Nakao, K. Suzuki, Y. Nakagawa, K. Tomishige, [Direct cyclic carbonate synthesis from CO₂ and diol over carboxylation/hydration cascade catalyst of CeO₂ with 2-cyanopyridine](#), ACS Catalysis, 4 (2014) 1893-1896.
- [25] J. Liu, Y. Li, J. Zhang, D. He, [Glycerol carbonylation with CO₂ to glycerol carbonate over CeO₂ catalyst and the influence of CeO₂ preparation methods and reaction parameters](#), Applied Catalysis A: General, 513 (2016) 9-18.
- [26] K. Phiwang, S. Suphankij, W. Mekprasart, W. Pecharapa, [Synthesis of CuO nanoparticles by precipitation method using different precursors](#), Energy Procedia, 34 (2013) 740-745.
- [27] J. Xu, W. Ji, Z. Shen, S. Tang, X. Ye, D. Jia, X. Xin, [Preparation and characterization of CuO nanocrystals](#), Journal of Solid State Chemistry, 147 (1999) 516-519.
- [28] V. Grover, R. Shukla, R. Kumari, B. Mandal, P. Kulriya, S. Srivastava, S. Ghosh, A. Tyagi, D. Avasthi, [Effect of grain size and microstructure on radiation stability of CeO₂: an extensive study](#), Physical Chemistry Chemical Physics, 16 (2014) 27065-27073.
- [29] D. Xue-yan, L. Wen-chao, L. Zhen-xiang, X. Kan, [X-ray photoelectron spectroscopy investigation of ceria doped with lanthanum oxide](#), Chinese physics letters, 16 (1999) 376.
- [30] A. Pfau, K. Schierbaum, [The electronic structure of stoichiometric and reduced CeO₂ surfaces: an XPS, UPS and HREELS study](#), Surface Science, 321 (1994) 71-80.
- [31] M. Škoda, M. Cabala, I. Matolínová, T. Skála, K. Veltruská, V. Matolín, [A photoemission study of the ceria and Au-doped ceria/Cu \(111\) interfaces](#), Vacuum, 84 (2009) 8-12.